

# Untwisting the Boerdijk-Coxeter Helix

Robert L. Read [read.robert@gmail.com](mailto:read.robert@gmail.com)

**Abstract.** The Boerdijk-Coxeter helix (BC helix, or tetrahelix) is a face-to-face stack of regular tetrahedra forming a helical column. Considering the edges of these tetrahedra as structural members, the resulting structure is attractive and inherently rigid, and therefore interesting to architects, mechanical engineers, and roboticists. A formula is developed that matches the visually apparent helices forming the outer rails of the BC helix. This formula is generalized to a formula convenient to designers. Formulae for computing the parameters that give edge-length minimax-optimal tetrahelices are given, defining a continuum of optimum tetrahelices of varying curvature. The endpoints of this continuum are the BC helix and a structure of zero curvature, the *equitetrabeam*. Numerically finding the rail angle from the equation for pitch allows optimal tetrahelices of any pitch to be designed. An interactive tool for such design and experimentation is provided: <https://pubinv.github.io/tetrahelix/>. A formula for the inradius of optimal tetrahelices is given. Utility for static and variable geometry truss/space frame design and robotics is discussed.

**Key words.** Boerdijk-Coxeter helix, tetrahelix, robotics, tetrobot, unconventional robots, structural engineering, mechanical engineering, tensegrity, variable-geometry truss

18 AMS subject classifications. 51M15

**1. Introduction.** The Boerdijk-Coxeter helix[3] (BC helix) (see Figures 1 and 2), is a face-to-face stack of tetrahedra that winds about a straight axis. Because architects, structural engineers, and roboticists are inspired by and follow such regular mathematical models but can also build structures and machines of differing or even dynamically changing length, it is useful to develop the mathematics of structures formed from tetrahedra where we relax regularity.

The vertices of the tetrahedra lie upon three helices about the central axis. The Tetrobot[11, 8] uses the regularity of this geometry to make a tentacle-like robot that can crawl like a slug or mollusc. These modular robotic systems use mechanical actuators which can change their length, connected by special joints, such as the 3D printable Song-Kwon-Kim[15] joint or the CMS joint[7] used in the original Tetrobot, which allow many members to meet in a single point. Such machines can follow purely regular mathematical models such as the Boerdijk-Coxeter helix or the Octet Truss[4].

32 Buckminster Fuller called the BC helix a *tetrahelix*[5], a term now commonly used. In this  
 33 paper we reserve *BC helix* to mean the purely regular structure and use *tetrahelix* to refer to  
 34 any structure isomorphic to the BC helix.

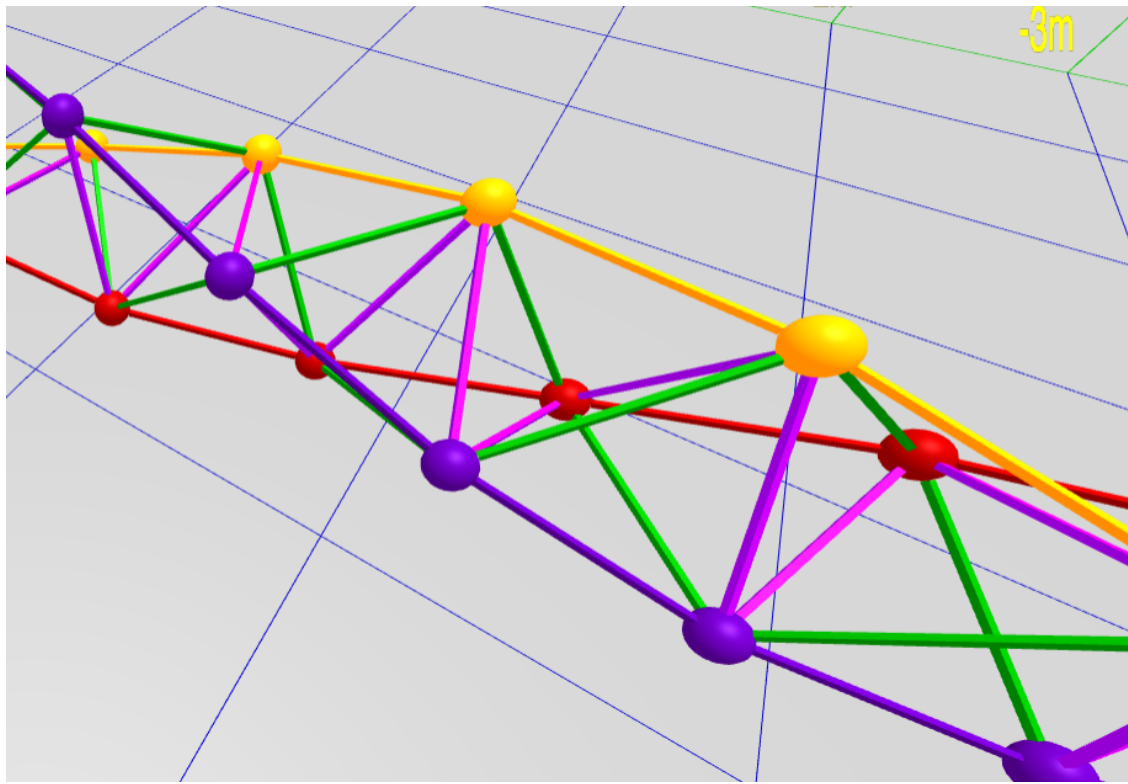


**Figure 1.** BC Helix Close-up (partly along axis)

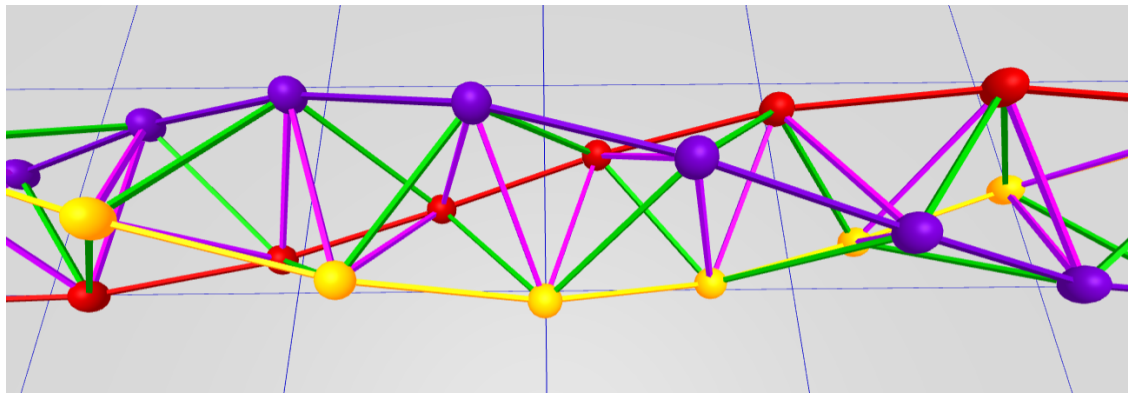


**Figure 2.** BC Helix Close-up (orthogonal)

35     Imagining Figures 1 and 2 as a static mechanical structure, we observe that it is useful  
 36 to the mechanical engineer or roboticist because the structure is an inherently rigid, omni-  
 37 triangulated space frame, which is mechanically strong. Then we can imagine that each static  
 38 edge is replaced with an actuator that can dynamically become shorter or longer in response  
 39 to electronic control, and the vertices are joints that support sufficient angular displacement

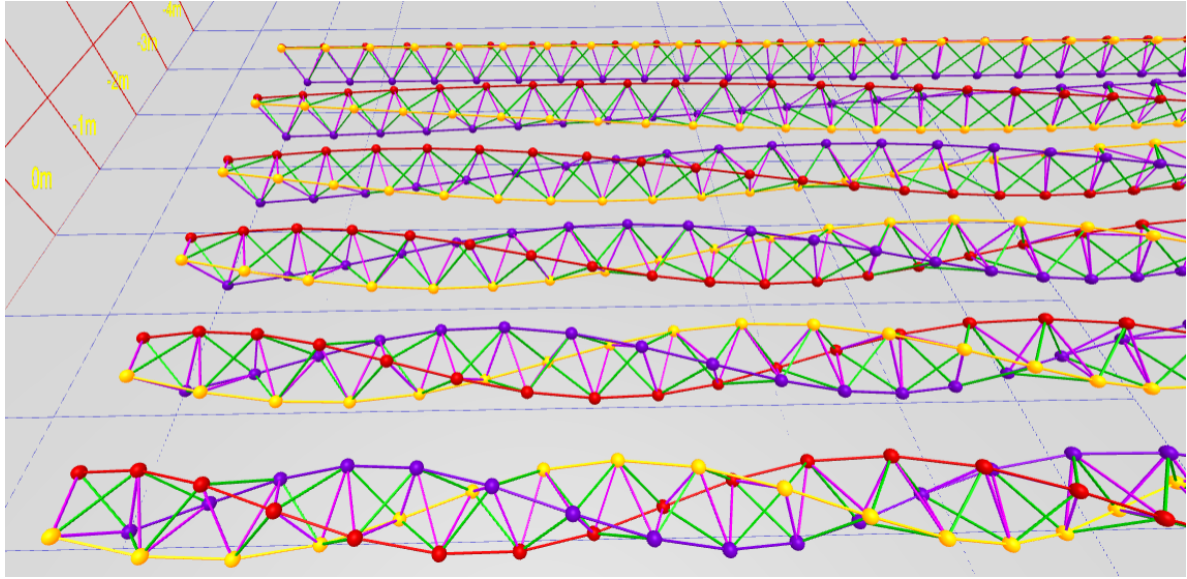


**Figure 3.** A Continuum of Tetrahelices

40 for this to be possible. An example of such a machine is a Tetrobot, shown in Figure 12.

41 A BC helix does not rest stably on a plane. It is convenient to be able to “untwist” it and  
 42 to form a tetrahelix space frame that has a flat planar surface. By making length changes in a  
 43 certain way, we can untwist a tetrahelix to form a *tetrabeam* which has planar faces and has,  
 44 for example, an equilateral triangular profile. This paper develops the equations needed to  
 45 untwist the tetrahelix. All math developed here is available in JavaScript and demonstrated by  
 46 an interactive design website <https://pubinv.github.io/tetrahelix/>[12], from which Figures 1  
 47 to 3, 7 and 8 are taken.

48 Figure 3 displays a continuum of tetrahelices optimal in a certain sense, which is the main  
 49 result of this paper. The closest helix is the BC helix, and the furthest is the equitetrabeam,  
 50 defined in section 6 and Figures 7 and 8.

51 **2. A Designer’s Formulation of the BC Helix.** We would like to design nearly regular  
 52 tetrahelices with a formula that gives the vertices in space. Eventually we would like to design  
 53 them by choosing the lengths of a small set of members. In a space frame, this is a static  
 54 design choice; in a tetrobot, it is a dynamic choice that can be used to twist the robot and/or  
 55 exert linear or angular force on the environment.

56 Ideally we would have a simple formula for defining the nodes based on any curvature or  
 57 pitch we choose. It is a goal of this paper to relate the Cartesian coordinate approach and  
 58 the member-length approach to generating a tetrahelix continuum.

59 H.S.M Coxeter constructs the BC helix[3] as a repeated rotation and translation of the  
 60 tetrahedra by showing the rotation is:

$$61 \quad \theta_{bc} = \arccos(-2/3)$$

62 and the translation:

$$63 \quad h_{bc} = 1/\sqrt{10}.$$

64 Note that  $\theta_{bc}$  is approximately  $0.37 \cdot 2\pi$  radians or 131.81 degrees. The angle  $\theta_{bc}$  is the  
65 rotation of *each* tetrahedron, not the tetrahedra along a rail. In [Figure 1](#), each tetrahedron  
66 has either a yellow, blue, or red outer edge or rail. That is, a blue-rail tetrahedron is rotated  
67 slightly more than a  $1/3$  of a revolution to match the face of the yellow tetrahedra.

68 R.W. Gray's website[\[6\]](#), repeating a formula by Coxeter[\[3\]](#) in a more accessible form, gives

69 the Cartesian coordinates  $\begin{bmatrix} x \\ y \\ z \end{bmatrix}$  for a counter-clockwise BC Helix in a right-handed coordinate  
70 system:

$$71 \quad (1) \quad \mathbf{V}(n) = \begin{bmatrix} r_{bc} \cos n\theta_{bc} \\ r_{bc} \sin n\theta_{bc} \\ nh_{bc} \end{bmatrix}, \text{ where: } \begin{aligned} r_{bc} &= \frac{3\sqrt{3}}{10} \approx 0.5196 \\ h_{bc} &= 1/\sqrt{10} \approx 0.3162 \\ \theta_{bc} &= \arccos(-2/3) \end{aligned}$$

72 and where  $n$  represents each integer numbered node in succession on every colored rail.

73 The apparent rotation of a vertex on an outer-edge, that is  $\mathbf{V}(n)$  relative from  $\mathbf{V}(n+3)$   
74 for any integer  $n$  in (1), is  $3\theta_{bc} - 2\pi$ .

75 This formula defines a helix, but it is not any of the apparent helices, or *rail* helices, of the  
76 BC helix, but rather one that winds much more rapidly through all nodes. To a designer of  
77 tetrahelices, it is more natural to think of the three helices which are visually apparent, that  
78 is, those three which are closely approximated by the outer edges or rails of the BC helix. We  
79 think of each of these three rails as being a different color: red, blue, or yellow. This situation  
80 is illustrated in [Figure 4](#), wherein the black helix represents that generated by (1), and the  
81 colored helices are generated by (2).

82 In order to develop the continuum of slightly irregular tetrahelices described in [section 7](#),  
83 we need a formula that gives us the nodes of just one rail helix, denoted by color  $c$  and integer  
84 node number  $n$ :

$$85 \quad (\forall n \in \mathbb{Z}, \forall c \in \{0, 1, 2\} : \mathbf{H}_{BCcolored}(n, c) = \mathbf{V}(3n + c)).$$

86 Such a helix can be written:

$$87 \quad (2) \quad \mathbf{H}_{BCcolored}(n, c) = \begin{bmatrix} r_{bc} \cos ((3\theta_{bc} - 2\pi)n + c\theta_{bc}) \\ r_{bc} \sin ((3\theta_{bc} - 2\pi)n + c\theta_{bc}) \\ 3h_{bc}(n + c/3) \end{bmatrix}, \text{ where } \begin{aligned} r_{bc} &= \frac{3\sqrt{3}}{10} \\ h_{bc} &= 1/\sqrt{10} \\ \theta_{bc} &= \arccos(-2/3) \end{aligned} .$$

88 In this formula, integral values of  $n$  may be taken as a node number for one rail and  
89 used to compute its Cartesian coordinates. Allowing  $n$  to take non-integer values defines a  
90 continuous helix in space which is close to the segmented polyline of the outer tetrahedra  
91 edges, and equals them at integer values.

92 [Figure 4](#) illustrates this difference with a 7-tetrahedra BC helix, which is in fact the same  
93 geometry as the robot illustrated in [Figure 12](#). Although the nodes coincide, (1) evaluated  
94 at real values generates the black helix which runs through every node, and (2) defines the

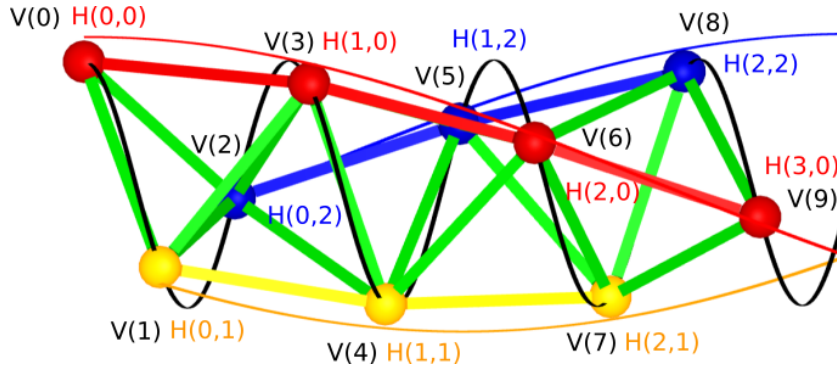


**Figure 4.** Rail helices ( $H$ ) vs. Coxeter/Gray helix ( $V$ )

95 red, yellow, and blue helices. (In this figure these rail helices have been rendered at a slightly  
96 higher radius than the nodes for clarity; in actuality the maximum distance between the  
97 continuous, curved helix and the straight edges between nodes is much smaller than can be  
98 clearly rendered.)

99 The quantity  $(3\theta_{bc} - 2\pi) \approx 35.43^\circ$  is the angular shift between  $\mathbf{V}(3n+c) = \mathbf{H}_{BCcolored}(n, c)$   
100 and  $\mathbf{V}(3(n+1)+c) = \mathbf{H}_{BCcolored}(n+1, c)$ . This quantity appears so often that we call it the  
101 “rail angle  $\rho$ ”. For the BC helix,  $\rho_{bc} = (3\theta_{bc} - 2\pi)$ .

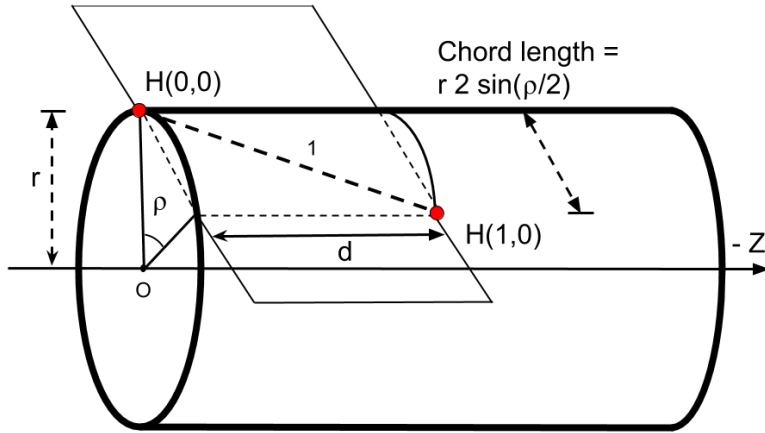


**Figure 5.** Rail Angle Geometry

102 Note in Figure 5 the  $z$ -axis travel for one rail edge is denoted by  $d$ . In (1) and (2),  
103 the variable  $h$  is used for one third of the distance we name  $d$ . We will later justify that  
104  $d = 3h$ . In this paper we assume the length of a rail is always 1 as a simplification, except in

105 proofs concerning rail length. (We make the rail length a parameter in our JavaScript code  
 106 in [https://github.com/PubInv/tetrahelix/blob/master/js/tetrahelix\\_math.js](https://github.com/PubInv/tetrahelix/blob/master/js/tetrahelix_math.js) [12].)

107 The  $\mathbf{H}_{BC\text{colored}}(n, c)$  formulation can be further clarified by rewriting directly in terms of  
 108 the rail angle  $\rho_{bc}$  rather than  $\theta_{bc}$ . Intuitively we seek an expression where  $c/3$  is multiplied by  
 109 a  $1/3$  rotation plus the rail angle  $\rho$ . We expand the expressions  $\theta_{bc}$  and  $\rho_{bc}$  in (2) and seek to  
 110 isolate the term  $c2\pi/3$ .

111 Thus, starting with the expression:

$$113 \quad c\theta_{bc}$$

114 we introduce 3 into the denominator...

$$115 \quad (c/3)(3\theta_{bc})$$

117 we want  $2\pi$  in numerator, so add canceling terms...

$$119 \quad (c/3)((3\theta_{bc} - 2\pi) + 2\pi)$$

120 ...and then use the definition of  $\rho_{bc}$

$$121 \quad (c/3)\rho_{bc} + c2\pi/3$$

123 finally using algebra, we obtain

$$124 \quad c(\rho_{bc} + 2\pi)/3.$$

126 This allows us to redefine:

$$127 \quad (3) \quad \mathbf{H}_{BC\text{colored}}(n, c) = \begin{bmatrix} r \cos \rho_{bc} n + c(\rho_{bc} + 2\pi)/3 \\ r \sin \rho_{bc} n + c(\rho_{bc} + 2\pi)/3 \\ (n + c/3)h_{bc} \end{bmatrix}, \text{ where } \begin{aligned} \rho_{bc} &= (3\theta_{bc} - 2\pi) \\ h_{bc} &= 1/\sqrt{10}. \end{aligned}$$

128 Recall that  $c \in \{0, 1, 2\}$ , but  $n$  is continuous (rational or real-valued.) We can now assert  
 129 that in Figure 4 the black helix winds at  $\frac{3\theta_{bc}}{\rho_{bc}} \approx 11.16$  times the rate of a rail helix.

130 From this formulation it is easy to see that moving one vertex on a rail ( $\mathbf{H}_{BC\text{colored}}(n, c)$ )  
 131 to  $\mathbf{H}_{BC\text{colored}}(n + 1, c)$  for any  $n$  and  $c$ ) moves us  $\rho_{bc}$  radians around a circle. Since:

$$132 \quad \frac{2\pi}{\rho_{bc}} \approx 10.16$$

133 we can see that there are approximately 10.16 red, blue or yellow tetrahedra on one rail in a  
 134 complete revolution of the tetrahelix.

135 The *pitch* of any tetrahelix, defined as the axial length of a complete revolution where  
 136  $\rho \neq 0$  is:

$$137 \quad (4) \quad p(\rho) = \frac{2\pi \cdot d}{\rho} .$$

138 The pitch of the Boerdijk-Coxeter helix of edge length 1 is the length of three tetrahedra  
139 times this number:

140                   
$$\frac{3h_{bc} \cdot 2\pi}{\rho_{bc}} = \frac{6\pi}{\sqrt{10}\rho_{bc}},$$
  
141

142 which is approximately 9.64.

143 The pitch is less than the number of tetrahedra because the tetrahedra edges are not  
144 parallel to the axis of the tetrahelix. It is a famous and interesting result that the pitch is  
145 irrational. A BC helix never has two tetrahedra at precisely the same orientation around the  
146  $z$ -axis. However, this is inconvenient to designers, who might prefer a rational pitch. The  
147 idea of developing a rational period by arranging solid tetrahedra by relaxing the face-to-  
148 face matching has been explored[13]. We develop below slightly irregular edge lengths that  
149 support, for example, a pitch of precisely 12 tetrahedra in one revolution which would allow  
150 an architect to design a pleasing column having the top and bottom tetrahedra in the same  
151 relationship to the capital and the basis to the viewer.

152 **3. Optimal Tetrahelices are Triple Helices.** We use the term *tetrahelix* to mean any  
153 structure physically constructible of vertices and finite edges which is isomorphic to the BC  
154 helix and in which the vertices lie on three helices. By isomorphic we mean there is a one-  
155 to-one mapping between both vertices and edges in the two tetrahelices. One could consider  
156 various definitions of optimality for a tetrahelix, but the most useful to us as roboticists  
157 working with the Tetrobot concept is to minimize the maximum ratio between any two edge  
158 lengths, because the Tetrobot uses mechanical linear actuators with limited range of extension.

159 A *triple helix* is three congruent helices that share an axis. We show that optimal tetra-  
160 helices are in fact triple helices with the same radius, so that all vertices are on a cylinder. In  
161 stages, we demonstrate that optimal tetrahelices:

- 162     1. have the same pitch,  
163     2. have parallel axes,  
164     3. share the same axis,  
165     4. have the same radius,  
166     5. have the same rail lengths,  
167     6. have axially equidistant nodes, and therefore  
168     7. are in fact triple helices.

169 Suppose that all three rails do not have the same pitch. If we start at any shortest edge  
170 between two rails, as we move from node to node away from our start edge the edge lengths  
171 between rails must always lengthen without bound, which cannot be optimal. So we are  
172 justified in talking about the *pitch* of the optimal tetrahelix as the pitch of its three rail  
173 helices, even though there are three such helices of equivalent pitch.

174 Similarly, if the axes are not parallel, there is an edge of unbounded length in the structure,  
175 so we do not consider such cases.

176 Define a *minimax edge-length optimal tetrahelix* or just an *optimal tetrahelix* to be a  
177 tetrahelix for which there exists no other tetrahelix with lower ratio of longest edge length to  
178 shortest edge length.

179 We wish to show that in an optimal tetrahelix, all vertices lie on the cylinder of radius  $r$ ,  
180 regardless of where they lie on the  $z$ -axis.

181 As a little lemma for the proof below, observe that a tetrahelix of zero radius, where all  
 182 points lie on the same line, is not as optimal as a tetrahelix of a small radius. The edges  
 183 between rails will be shorter than the rail edges, and moving them apart slightly lengthens  
 184 the between-edge rails, improving the ratios.

185 In the proof below we find useful to consider projection diagrams that are the axial pro-  
 186 jection of a tetrahelix onto the  $XY$ -plane. [Figure 10](#) is an example of such a diagram.

187 **Lemma 1.** *If the rail angle  $0 < \rho < \pi$  is a rational multiple of  $\pi$ , then the projection of  
 188 edges in a helix of that rail angle along the  $z$ -axis onto the  $XY$ -plane form a regular polygon  
 189 of 3 or more sides, or else they fill in a complete circle.*

190 *Proof.* All points lying on a helix projected along the axis lie on a circle in the  $XY$ -plane.  
 191 Helices are periodic in the  $z$  dimension modulo  $2\pi$ . If  $2\pi/\rho$  is irrational, the projection onto  
 192 the  $XY$ -plane will contain an unbounded number of points on a circle. If and only if  $2\pi/\rho$   
 193 is rational, the projection onto the  $XY$ -plane will contain a finite number of points. Because  
 194  $\pi$  is transcendental and irrational,  $2\pi/\rho$  is rational if and only  $\rho = a\pi/b$ , where  $a$  and  $b$  are  
 195 integers and without loss of generality  $a$  and  $b$  are coprime. Since  $\rho < \pi$ , therefore  $a < b$ .  
 196 Also,  $\rho > 0$ , therefore  $a > 0$ . The number of points in the projection is  $2b$  if  $a$  is odd, and  $b$  if  
 197  $a$  is even. This polygon has at least 3 sides, since either  $\rho$  is irrational or  $b > a$ , and therefore  
 198  $b \geq 2$ . If  $a/b = 1/2$ , the projection is a square, which has four sides. ■

199 **Theorem 2.** *Any optimal tetrahelix with a rail angle of magnitude less than  $\pi$  has all three  
 200 axes coincident.*

201 *Proof.* Case 1: Suppose that  $\rho$  is zero. Each helix has zero curvature, that is, it is a  
 202 straight line. These lines are equivalent to some three degenerate helices with coincident axes,  
 203 possibly with different radii, so long as there is a phase term in the definition of the helix, as  
 204 in [\(2\)](#). We later show the radii must be equivalent.

205 Case 2: Suppose that  $\rho$  is positive but less than  $\pi$ . In this case each rail helix has curvature.  
 206 The projection of points in the  $XY$  plane creates a figure guaranteed to have points on either  
 207 side of any line through the axis of such a helix, because the figure is either an  $n$ -gon or a  
 208 circle by [Lemma 1](#). We show that the three helices share a common axis.

209 Without loss of generality define the Red helix to have its axis on the  $z$ -axis. Since there  
 210 must be at least one Red-to-Yellow or a Red-to-Blue edge that is either a minimum or a  
 211 maximum, without loss of generality define the Blue helix to be a helix that has an edge  
 212 connection to the Red helix that is either a maximum or a minimum. Let  $B'$  be a translation  
 213 in the  $XY$ -plane of the blue helix  $B$  so that its axis is the  $z$ -axis and coincident with the red  
 214 helix  $R$ . Let  $D$  be the distance between the axis of the Blue helix  $B$  and  $B'$ . We will show  
 215 that if  $D > 0$  then  $B$  “wobbles” in a way that cannot be optimal. Define a wobble vector by:

$$216 \quad \mathbf{W}(n) = \mathbf{B}(n) - \mathbf{B}'(n) .$$

217 where  $\mathbf{B}(n)$  and  $\mathbf{B}'(n)$  is the vector  $\begin{bmatrix} x \\ y \end{bmatrix}$  for the projection of the  $n$ th vertex of  $B$  and  $B'$ .  
 218 Note that  $\|\mathbf{R}(n) - \mathbf{B}'(n+k)\|$  (the Euclidean distance of the vertices) is a constant for any  $k$ ,  
 219 because  $R$  and  $B'$  have the same pitch and the same axis, even if they do not have the same  
 220 radius.

221     Figure 6 illustrates this situation. Like most diagrams, it is over specific, in that the two  
 222 circles are drawn of the same radius but we do not depend upon that in this proof. The  
 223 diagram represents the projection along the  $z$  axis of a few points into the  $XY$ -plane.

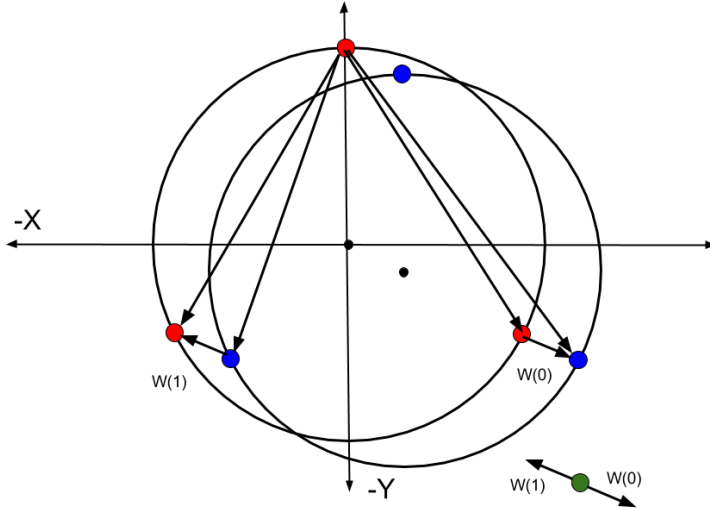


**Figure 6.** Wobble Vectors from Non-Coincident Axes

224     Since  $\rho < \pi$  by assumption, by [Lemma 1](#), the set of wobbles  $\{\mathbf{W}(n)|\text{for any } n\}$  contains  
 225 at least three vectors, at least two of which pointing in different directions. For any point not  
 226 at the origin, at least one of these vectors moves closer to the point and at least one moves  
 227 further away.

228     The set of all lengths in the tetrahelix is a superset of:  $L = \{||\mathbf{R}(n) - \mathbf{B}(n)||\}$ , which  
 229 by our choice has at least one longest or shortest length. (Note this is just the Euclidean  
 230 distance formula written as a Euclidean norm.)  $L = \{||\mathbf{R}(n) - (\mathbf{B}'(n) + \mathbf{W}(n))||\}$  and so  
 231  $L = \{||(\mathbf{R}(n) - \mathbf{B}'(n)) - \mathbf{W}(n)||\}$ . But  $\mathbf{R}(n) - \mathbf{B}'(n)$  is a constant, so the minimax value of  
 232  $L$  is improved as  $||\mathbf{W}(n)||$  decreases. By our choice that there is a Blue-to-Red edge that is  
 233 either a maximum or a minimum, this improves the minimax value of the total tetrahelix.

234     This process can be carried out on both the Blue and Yellow helices (perhaps simultane-  
 235 ously) until  $\mathbf{W}(n)$  is zero for both, finding a tetrahelix of improved overall minimax value at  
 236 each step. So a tetrahelix is optimal only when  $\mathbf{W}(n) = 0$ , and therefore when  $D = 0$  and  
 237  $\mathbf{B}(n) = \mathbf{B}'(n)$ , and all three axes are coincident. ■

238     Now that we have shown that axes are coincident and parallel and that the pitches are  
 239 the same for all helices, we can assert that any optimum tetrahelix can be generated with an

240 equation for helices:

241 (5)  $\mathbf{V}_{\text{triple}}(n, c) = \begin{bmatrix} r_c \cos(n\alpha + c2\pi/3 + \phi_c) \\ r_c \sin(n\alpha + c2\pi/3 + \phi_c) \\ \frac{d(n+c/3)}{3} \end{bmatrix}$ , where:  $c \in \{0, 1, 2\}$

242 which would be much more complicated if the axes were not coincident. Note that we have  
 243 not yet shown that the relationships of the radius  $r_c$  or the phase  $\phi_c$  for the three helices, so we  
 244 denoted them with a  $c$  subscript to show they are dependent on the color. We have not yet  
 245 investigated in the general case the relationships between  $\alpha, r, \phi$  and  $d$  in (5). In section 4 we  
 246 give a more specific version of this formula which generates optimal tetrahelices. We observe  
 247 that when  $\alpha = 0$ , the helices are degenerate, having curvature of 0, but because of the  $\phi_c$   
 248 term, they are not collinear.

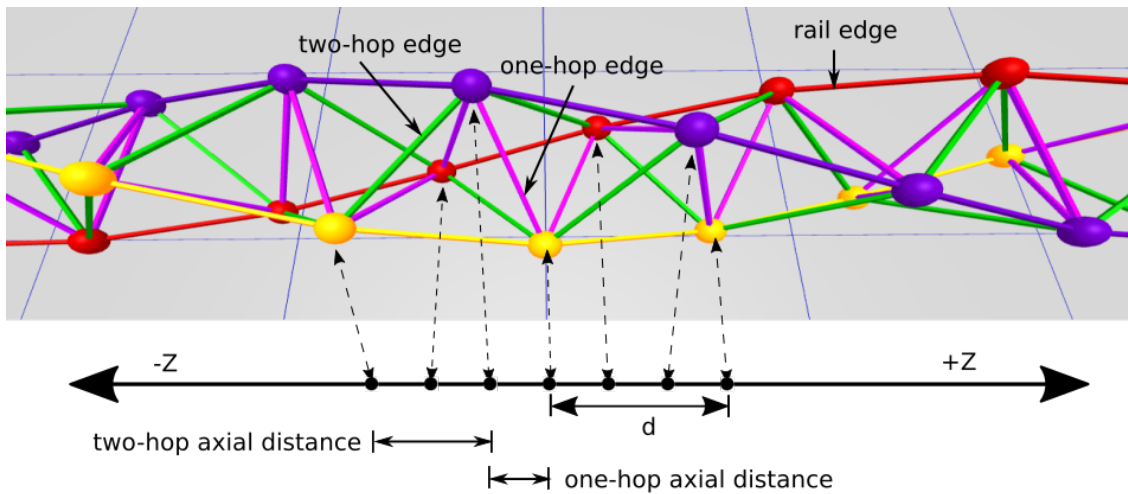


Figure 7. Edge Naming

249 In principle any three helices generated with (5) has at most nine distinct edge length  
 250 classes. Each edge that connects two rails potentially has a longer length and shorter length  
 251 we denote with a + or -. So the classes are  $\{RR, BB, YY, RB_+, RB_-, BY_+, BY_-, RY_+, RY_-\}$ .  
 252 If when projecting all vertices onto the  $z$ -axis (dropping the  $x$  and  $y$  coordinates), the interval  
 253 defined by the  $z$  axis value of its endpoints contains no other vertices, we call it a *one-hop*  
 254 edge, and if it does contain another vertex we call it a *two-hop* edge, as illustrated in Figure 7.  
 255 Then there are 3 rail edges  $\{RR, BB, YY\}$ , 3 one-hop lengths  $\{RB_-, BY_-, RY_-\}$  between  
 256 each pair of 3 rails, and 3 two-hop lengths  $\{RB_+, BY_+, RY_+\}$  between each pair of 3 rails,  
 257 where the two-hop length is at least the one-hop length. However, if we generate the three  
 258 helices symmetrically with (5), many of these lengths will be the same. In fact, it is possible  
 259 that there will be only two distinct such classes, or even one, in the purely regular BC helix.

260 **Theorem 3.** *Optimal tetrahelices have the same radii for all three helices.*

261     *Proof.* To prove this we exhibit a symmetric tetrahelix (not yet shown to be optimal)  
 262 which happens to be a triple helix, that has the property that all rail edges are equal to all  
 263 one-hop edges and all two-hop edges are equal to each other. Observe that although we have  
 264 not yet given the formula for the radii of such a triple helix, we observe there are some values  
 265 for  $r$  and  $\alpha$ , and  $\phi$  in (5) for which all the three helices are symmetrically and evenly spaced.  
 266 Furthermore, we can choose these values such that the three rail edges are of length 1 and so  
 267 that the one-hop lengths are also all of length 1, and the two-hop lengths are slightly longer.

268     Now consider a tetrahelix in which the radius of one of the helices is different. By the  
 269 connections made in a tetrahelix, any increase to a radius increases both a one-hop and two-  
 270 hop distance, and any decrease likewise decreases two. Since there exists a tetrahelix which  
 271 has only two distinct classes of edge lengths, (the smaller being one-hop = rail, the larger  
 272 being the two-hop distance), the helix with a larger radius increases a longest edge without  
 273 increasing a shortest edges. Likewise, a helix with a smaller radius decreases a one-hop edge  
 274 without decreasing a two-hop edge. Therefore, a tetrahelix with different radii is not as  
 275 optimal as some two-class tetrahelix generated by (5), and so it is not optimal. We have not  
 276 yet proved that a two-class tetrahelix is optimal, but it suffices to show that there exist such  
 277 a better tetrahelix to show that different radii imply a suboptimal tetrahelix. ■

278     Because an optimal tetrahelix has equivalent radii and equivalent pitch for all three helices,  
 279 it has equivalent rail edge lengths. Likewise, there is a single rail angle  $\rho$  that represents the  
 280 rotation of two nodes connected by a single rail edge, and it is the same for all three rails.

281     Now that we have shown that on any optimal tetrahelix the vertices are on helices of the  
 282 same axes and pitch, we see that the vertices of any optimal tetrahelix will lie on a cylinder,  
 283 or a circle when the axis dimension is projected out. Therefore it is reasonable to now speak  
 284 of the singular *radius*  $r$  of a tetrahelix as the radius of the cylinder. We can now go on to the  
 285 harder proof about where vertices occur along the  $z$ -axis.

286     We show that in fact the nodes must be distributed in even thirds along the  $z$ -axis, as in  
 287 fact they are in the regular BC helix.

288     However, we have already shown the rail lengths are equal in any optimal tetrahelix.

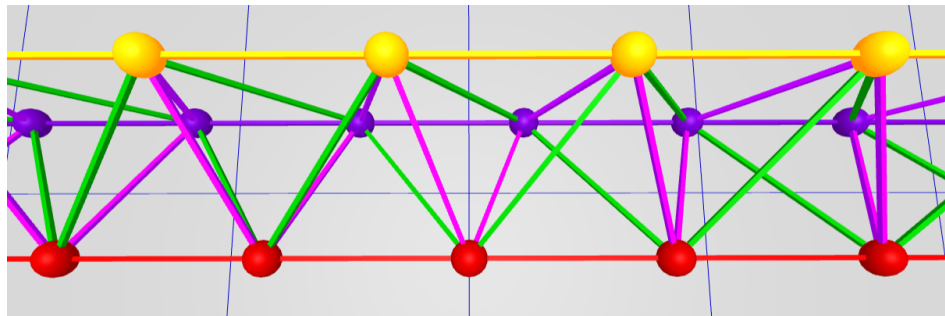


**Figure 8.** Equitetrabeam

289     Figure 8 shows the equitetrabeam, which is defined in section 6, but also conveniently  
 290 illustrates the one-hop and two-hop edge definitions. The green edges are the two-hop edges  
 291 and the purple edges are the one-hop edges. Note that the green edges are slightly longer than

292 the purple edges. In [Figure 7](#), which depicts the BC helix, the two-hop and one-hop edges are  
293 of equal length (but the projection onto the  $z$ -axis, the axial length, of the two-hop edge is  
294 longer than the axial one-hop length.)

295 **Theorem 4.** *An optimal tetrahelix of any rail angle  $\rho < \pi$  is a triple helix with all vertices  
296 evenly spaced at  $d/3$  intervals on the  $z$  axis. Any one tetrahedron in a tetrahelix has 1 rail  
297 edge, 2 one-hop edges connected to the rail and 2 two-hop edges connected to the rail. The  
298 sixth edge is opposite of the rail edge and is a one-hop edge.*

299 **Proof.** Consider a tetrahelix in which the vertices are evenly spaced at  $d/3$  intervals on  
300 the  $z$  axis. Every edge is either a rail edge, or it makes one hop, or two hops. All of the  
301 one-hop edges are equal length. All of the two-hop edges are equal length.

302 Every vertex is connected to 4 non-rail edges. There is a one-hop edge in both the positive  
303 and negative  $z$  direction. Likewise there is a two-hop edge in both the positive and negative  
304  $z$  direction. Let  $A$  be the set of edge lengths, which has only 3 members, represented by  
305  $A = \{o, t, r\}$  for the one-hop, two-hop, and rail edge lengths.

306 Any attempt to perturb any rail in either  $z$  direction lengthens one two-hop edge to  $t'$ ,  
307 where  $t' > t$  and shortens one one-hop edge  $o' < o$ . Let  $B = \{o', t'\} \cup A$  be the edge lengths of  
308 such a perturbed tetrahelix. The minimax of  $B$  is greater than the minimax of  $A$  since there  
309 is a single rail length which cannot be both greater than  $t'$  and  $o'$  and less than  $t'$  and  $o'$ .  
310 Therefore, any optimal tetrahelix has all one-hop edges between all rails equal to each other,  
311 and all two-hop edges equal to each other, the  $z$  distances between rails equal. Therefore  
312 vertices are  $d/3$  from each other on the  $z$ -axis. ■

313 Note that based on [Theorem 4](#), there are only 3 possible lengths in an optimal tetrahelix,  
314 and we are justified in classifying edge lengths as *rail*, *one-hop*, or *two-hop*. The one-hop edges  
315 are the edges between rails that are closest on the  $z$ -axis, and the two-hop edges are those  
316 that skip over a vertex.

317 Taking all of these results together, each helix in an optimal tetrahelix is congruent to the  
318 others, shares an axis, is the same radius, and are evenly spaced axially. An optimal tetrahelix  
319 is therefore a *triple helix*, of a radius we have not yet demonstrated.

320 **4. Parameterizing Tetrahelices via Rail Angle.** We seek a formula to generate optimal  
321 tetrahelices that accepts a parameter that allows us to design the tetrahelix conveniently.  
322 Please refer back to [Figure 5](#). The pitch of the helix is an obvious choice, but is not defined  
323 when the curvature is 0, an important special case. The radius or the axial distance between  
324 two nodes on the same rail are possible choices, but perhaps the clearest choice is to build  
325 formulae that takes as their input the “rail angle”  $\rho$ . We define  $\rho$  to be the angle formed in  
326 the X,Y plane  $\angle \mathbf{H}(0,0)O\mathbf{H}(0,1)$  projecting out the  $z$  axis and sighting along the positive  $z$   
327 axis. In other words,  $\rho$  controls how far a rail edge of a tetrahelix deviates from being parallel  
328 with the axis, or the “twistiness” of the tetrahelix. We use the parameter  $\chi = 1$  to indicate a  
329 chirality of counter-clockwise, and  $\chi = -1$  for clockwise. We take our coordinate system to  
330 be right-handed.

331 The quantities  $\rho, r, d$  (see [Figure 5](#)) are related by the expression:

332  $1^2 = d^2 + (2r \sin \rho/2)^2$ , or  
 333 (6)  $d^2 = 1 - 4r^2(\sin \rho/2)^2$ .

334

335 Checking the important special case of the BC helix, we find that this equation indeed  
 336 holds true, treating  $d$  in this equation as  $3h_{bc}$  as defined by Gray and Coxeter, that is,  $d_{bc} =$   
 337  $3h_{bc}$ , where they are using  $h$  for the axial height from one node to the next of a different color,  
 338 but we use  $d$  to mean distance between nodes of the same color.

339 The rail angle  $\rho$  also has the meaning that  $2\pi/\rho$  is the number of tetrahedra in a full  
 340 revolution of the helix.

341 In choosing  $\rho$ , one greatly constrains  $r$  and  $d$ , but does not completely determine both of  
 342 them together, so we treat both as additional parameters.

343 Rewriting our formulation in terms of  $\rho$ :

344 (7) 
$$\mathbf{H}_{general}(\chi, n, c, \rho, d_\rho, r_\rho) = \begin{bmatrix} r_\rho \cos(\chi \cdot (n\rho + c(\rho + 2\pi)/3)) \\ r_\rho \sin(\chi \cdot (n\rho + c(\rho + 2\pi)/3)) \\ d_\rho(n + c/3) \end{bmatrix}$$

345 where:  $1 = d_\rho^2 + 4r_\rho^2(\sin \rho/2)^2$   
 346  $\chi \in \{-1, 1\}$ .

347  $\mathbf{H}_{general}$  forces the user to select three values:  $\rho$ ,  $r_\rho$ , and  $d_\rho$  satisfying (6).  
 348 Note that when  $\rho = 0$  then  $d_\rho = 1$ , but  $r_\rho$  is not determined by (6).

349 **Theorem 5.** For rail angles of magnitude at most  $\rho_{bc}$ , tetrahelices generated by  $\mathbf{H}_{general}$   
 350 are optimal in terms of minimum maximum ratio of member length when radius is chosen so  
 351 that the length of the one-hop edge is equal to the rail length.

352 **Proof.** By Theorem 4, we can compute the (at most) three edge-lengths of an optimal  
 353 tetrahelix by formula universally quantified by  $n$  and  $c$ :

354  $\text{rail} = \|\mathbf{H}_{general}(n, c, \rho, d_\rho, r) - \mathbf{H}_{general}(n+1, c, \rho, d_\rho, r)\| = 1$   
 355  $\text{one-hop} = \|\mathbf{H}_{general}(n, c, \rho, d_\rho, r) - \mathbf{H}_{general}(n, c+1, \rho, d_\rho, r)\|$  and,  
 356  $\text{two-hop} = \|\mathbf{H}_{general}(n, c, \rho, d_\rho, r) - \mathbf{H}_{general}(n, c+2, \rho, d_\rho, r)\|$ .

357

358 This syntax just represents the Euclidean distance formula. Thus:

359  $\text{one-hop} = \|\mathbf{H}_{general}(n, c, \rho, d_\rho) - \mathbf{H}_{general}(n, c+1, \rho, d_\rho)\|$

360

361 so:

362 
$$\text{one-hop} = \sqrt{\frac{d_\rho^2}{9} + r^2(\sin^2(\rho/3 + \frac{2\pi}{3}) + (1 - \cos(\rho/3 + \frac{2\pi}{3}))^2)}$$

363

368 but:  $d_\rho^2 = 1 - 4r^2(\sin(\rho/2)^2)$ , so we substitute:

$$369 \quad \text{one-hop} = \sqrt{\frac{1}{9} + r^2\left(-\frac{4(\sin^2(\rho/2))}{9} + \sin^2(\rho/3 + \frac{2\pi}{3}) + (1 - \cos(\rho/3 + \frac{2\pi}{3}))^2\right)}.$$

370

372 By similar algebra and trigonometry:

$$373 \quad \text{two-hop} = \sqrt{\frac{4}{9} + r^2\left(-\frac{16(\sin^2(\rho/2))}{9} + \sin^2(2\rho/3 + \frac{4\pi}{3}) + (1 - \cos(2\rho/3 + \frac{4\pi}{3}))^2\right)}.$$

374

376 By definition of minimax edge length optimality, we are trying to minimize:

$$377 \quad \frac{\max \{1, \text{one-hop}(r), \text{two-hop}(r)\}}{\min \{1, \text{one-hop}(r), \text{two-hop}(r)\}}.$$

378 But since  $\text{two-hop}(r) \geq \text{one-hop}(r)$ , this is equivalent to:

$$379 \quad \frac{\max \{1, \text{two-hop}(r)\}}{\min \{1, \text{one-hop}(r)\}}.$$

380 This quantity will be equal to one of:

$$381 \quad (8) \quad \frac{\text{two-hop}(r)}{1}, \frac{1}{\text{one-hop}(r)}, \frac{\text{two-hop}(r)}{\text{one-hop}(r)}.$$

382 We know that both  $\text{one-hop}(r)$  and  $\text{two-hop}(r)$  increase monotonically and continuously  
383 with increasing  $r$ . By inspection it seems likely that we will minimize this set by equating  
384  $\text{one-hop}(r)$  or  $\text{two-hop}(r)$  to 1, but to be absolutely sure and to decide which one, we must  
385 examine the partial derivative of the ratio  $\frac{\text{two-hop}(r)}{\text{one-hop}(r)}$  in this range.

386 Although complicated, we can use Mathematica to investigate the partial derivative of  
387 the  $\frac{\text{two-hop}(r)}{\text{one-hop}(r)}$  with respect to the radius to be able to understand how to choose the radius to  
388 form the minimax optimum.

389 Let:

$$390 \quad f_\rho = -\frac{4(\sin^2(\rho/2))}{9},$$

391

$$392 \quad g_\rho = -\frac{16(\sin^2(\rho/2))}{9},$$

393

$$394 \quad j_\rho = \sin^2(\rho/3 + \frac{2\pi}{3}) + (1 - \cos(\rho/3 + \frac{2\pi}{3}))^2,$$

395 and:

$$396 \quad k_\rho = \sin^2(2\rho/3 + \frac{4\pi}{3}) + (1 - \cos(2\rho/3 + \frac{4\pi}{3}))^2.$$

397 Then:

$$398 \quad \frac{\text{two-hop}(r)}{\text{one-hop}(r)} = \frac{\sqrt{\frac{4}{9} + r^2(g_\rho + j_\rho)}}{\sqrt{\frac{1}{9} + r^2(f_\rho + k_\rho)}}.$$

399

400 By graph inspection using Mathematica (<https://github.com/PubInv/tetrahelix/blob/master/tetrahelix.nb>), we see the partial derivative of this with respect to radius  $r$  is always negative, for any  $\rho \leq \rho_{bc}$ . (When the rail angle approaches  $\pi$ , corresponding to going almost to the other side of the tetrahelix, this is not necessarily true, hence the limitation in our statement of the theorem is meaningful.) Since the partial derivative of  $\frac{\text{two-hop}(r)}{\text{one-hop}(r)}$  with respect to the radius  $r$  is negative for all  $\rho$  up until  $\rho_{bc}$ , this ratio goes down as the radius goes up, and we minimize the maximum edge-length ratio by choosing the largest radius up until one-hop = 1, the rail-edge length. If we attempted to increase the radius further we would not be optimal, because the ratio  $\frac{\text{two-hop}(r)}{1}$  would become the largest ratio in our set of ratios (8).

410 Therefore we decrease the minimax length of the whole system as we increase the radius  
411 up to the point that the shorter, one-hop distance is equal to the rail-length, 1. In order to  
412 optimize the whole system so long as  $\rho \leq \rho_{bc}$ , we equate one-hop to 1 to find the optimum  
413 radius:

$$414 \quad 1 = \sqrt{\frac{1}{9} + r_{opt}^2 \left( -\frac{4(\sin^2(\rho/2))}{9} + \sin^2(\rho/3 + \frac{2\pi}{3}) + (1 - \cos(\rho/3 + \frac{2\pi}{3}))^2 \right)}, \text{ so...}$$

415 (9)  $r_{opt} = \frac{2}{\sqrt{\frac{9}{2} \cdot (\sqrt{3}\sin(\rho/3) + \cos(\rho/3)) + \cos(\rho) + 8}}.$

416

418 We can now give a formula for  $d_{opt}$  computed from  $\rho, r_{opt}$  via the rail angle equation (6):

$$419 \quad d_{opt}^2 = 1 - 4 \left( \frac{2}{\sqrt{\frac{9}{2} \cdot (\sqrt{3}\sin(\rho/3) + \cos(\rho/3)) + \cos(\rho) + 8}} \right)^2 (\sin(\rho/2))^2$$

420  $d_{opt}^2 = 1 - \frac{16(\sin(\rho/2))^2}{9(\sqrt{3}\sin(\rho/3) + \cos(\rho/3)) + \cos(\rho) + 8}$

421 (10)  $d_{opt} = \sqrt{1 - \frac{16\sin^2(\rho/2)}{\cos(\rho) + 9(\sqrt{3}\sin(\rho/3) + \cos(\rho/3)) + 8}}.$

422

424 Thus, by computing  $r_{opt}$  and  $d_{opt}$  as a function of  $\rho$  from this equation, we can construct  
425 minimax optimal tetrahelix for an  $0 \leq \rho \leq \rho_{bc}$ . ■

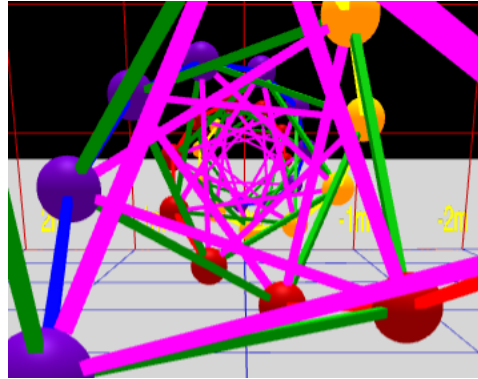


**Figure 9.** Axial view of a BC-Helix

**5. The Inradius.** Since the axes are parallel, we may define the *inradius*, represented by the letter  $i$ , of a tetrahelix to be the radius of the largest cylinder parallel to this axis that is surrounded by each tetrahelix and penetrated by no edge.

If we look down the axis of an optimal tetrahelix as shown in Figure 9, it happens that only the one-hop edges (rendered in purple in our software) comes closest to the axis. In other words, they define the radius of the incircle of the projection, or the radius of a cylinder that would just fit inside the tetrahelix. A formula for the inradius of the tetrahelix is useful if you are designing it as a structure that bears something internally, such as a firehose, a pipe, or a ladder for a human. The inradius  $r_{in}(\rho)$  of an optimal tetrahelix is a remarkably simple function of the radius  $r$  and the rail angle  $\rho$ :

$$436 \quad (11) \qquad r_{in}(\rho) = r \sin \frac{\pi - \rho}{6} ,$$

which can be seen from the trigonometry of a diagram of the projected one-hop edges connecting four sequentially numbered vertices:

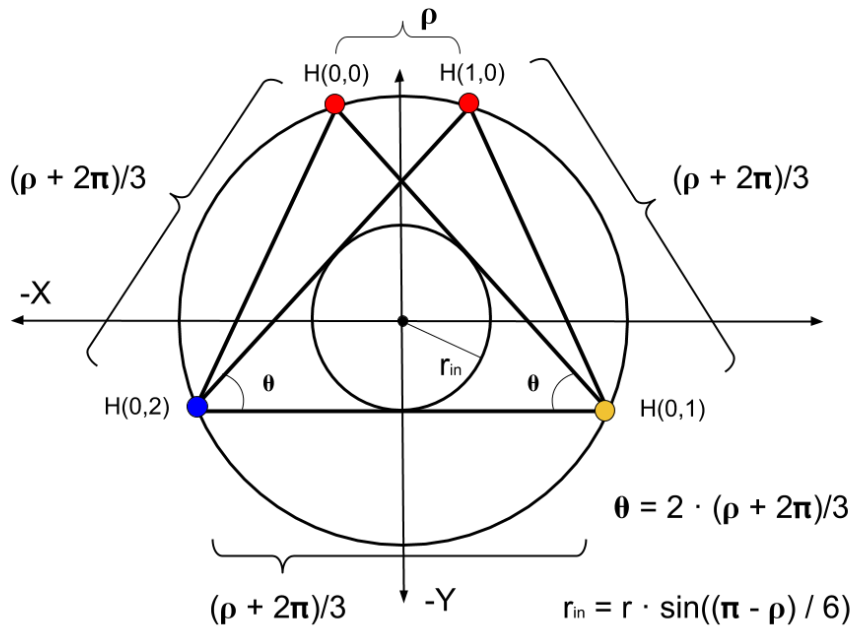


**Figure 10.** General One-hop Projection Diagram

From this equation with the help of symbolic computation we observe that inradius of the BC helix of unit rail length is  $r_{in(\rho_{bc})} = \frac{3}{10\sqrt{2}} \approx 0.21$ .

**6. The Equitetrabeam.** Just as  $\mathbf{H}_{\text{general}}$  constructs the BC helix (with careful and non-obvious choices of parameters) which is an important special case due to its regularity, it constructs an additional special (degenerate) case when the rail angle  $\rho = 0$  and  $d = 1$  (the edgelength), where the cross sectional area is an equilateral triangle of unchanging orientation, as shown in Figure 8 and at the rear of Figure 3. We call this the *equitetrabeam*. It is not possible to generate an equitetrabeam from (1) without the split into three rails introduced by (2) and completed in (7).

**Corollary 6.** The equitetrabeam with minimal maximal edge ratio is produced by  $\mathbf{H}_{\text{general}}$  when  $r = \sqrt{\frac{8}{27}}$ .

*Proof.* Choosing  $d = 1$  and  $\rho = 0$  we use Equation (9) to find the radius of optimal minimax difference.

### 452 Substituting into (7):

$$\text{one-hop} = \sqrt{\frac{1}{9} + 3r^2}$$

456 Then:

457 
$$1 = \sqrt{\frac{1}{9} + 3r^2}$$
 solved by...

458 
$$r = \sqrt{\frac{8}{27}}$$
  $\approx 0.54$

459

460 This radius<sup>1</sup> produces a two-hop rail length of  $\frac{2}{\sqrt{3}}$ . The difference between this and 1 is  
 461  $\approx 15.47\%$ . The inradius of the equitetrabeam of unit rail length from both Equation (11) and  
 462 the fact that the inradius of an equilateral triangle is half the circumradius is  $\sqrt{\frac{8}{27}}/2$ , or  $\frac{\sqrt{6}}{9}$ .

463 In Figure 3, the furthest tetrahelix is the optimal equitetrabeam. Figure 8 is a closeup of  
 464 an equitetrabeam.

465 To the extent that we value tetrabeams (that is, tetrahelices with a rail angle of 0, and  
 466 therefore zero curvature) as mathematical or engineering objects, we have motivated the  
 467 development of  $\mathbf{H}_{general}$  as a transformation of  $\mathbf{V}(n)$  defined by Equation (1) from Gray and  
 468 Coxeter. It is difficult to see how the  $\mathbf{V}(n)$  formulation could ever give rise to a continuum  
 469 producing the tetrabeam, since setting the angle in that equation to zero can produce only  
 470 collinear points.

471 The equitetrabeam may possibly be a novel construction. The fact that 6 members meet  
 472 in a single point would have been a manufacturing disadvantage that may have dissuaded  
 473 structural engineers from using this geometry. However, the advent of additive manufacturing,  
 474 such a 3D printing, and the invention of two distinct concentric multimember joints[15, 7] has  
 475 improved that situation.

476 Note that the equitetrabeam has chirality, which becomes important in our attempt to  
 477 build a continuum of tetrahelices.

478 **7. An Untwisted Continuum.** We observe that Equations (9) and (10) compute  $r_{opt}$   
 479 and  $d_{opt}$  which create an optimal tetrahelix for any rail angle  $\rho$  between 0, which gives the  
 480 equitetrabeam and  $\rho_{bc} \approx 35.43^\circ$ , which gives the BC helix.

481 Because the equitetrabeam which has a rail angle of 0 still has chirality, that is, one still  
 482 must decide to connect the one-hop edge to the clockwise or the counter-clockwise node, it is  
 483 not possible to build a smooth continuum where  $\rho$  transitions from positive to negative which  
 484 remains optimal. One can use a negative  $\rho$  in  $\mathbf{H}_{general}$  but it does not produce minimax  
 485 optimal tetrahelices. In other words, untwisting a counter-clockwise tetrahelix to rail angle  
 486 0 and then going even further does produce a clockwise tetrahelix, but one in which the  
 487 one-hop and two-hop lengths in the wrong places, that is, two-hop becomes shorter than one-  
 488 hop. Likewise,  $\rho > \rho_{bc}$  generates a tetrahelix, but minimax optimality is not guaranteed by  
 489  $\mathbf{H}_{general}$ .

490 The pitch of a helix for a fixed  $z$ -axis travel  $d$  is trivial (see (4)). However, if one is  
 491 computing  $z$ -axis travel from (10) the pitch is not simple. It increases monotonically and  
 492 smoothly with decreasing  $\rho$ , so (4) can be easily solved numerically with a Newton-Raphson

---

<sup>1</sup>Another interesting but non-optimal solution is derived by setting  $(\text{one-hop} + \text{two-hop})/2 = 1$ , occurs at  $r = \sqrt{35}/4$  which produces three length classes of  $11/12, 12/12, 13/12$ .

494 solver, as we do on our website. For a pitch at least  $p \geq \frac{3\sqrt{2}\pi}{\sqrt{5}\rho_{bc}} \approx 9.64$ , using (10) produces  
495 minimax optimal tetrahelices.

496 In this way a rail angle can be chosen for any desired (sufficiently large) pitch, yielding  
497 the optimum radius, the one-hop length, and the two-hop length that an engineer needs to  
498 construct a physical structure.

499 The curvature of a rail helix is formally given by:

500 (12) 
$$\frac{|r_\rho|}{r_\rho^2 + (d_\rho/\rho)^2} .$$

501 which goes to 0 as  $\rho$  approaches 0 (the equitetrabeam.) As  $\rho$  increase up to  $\rho_{bc}$  the curvature  
502 increases smoothly until the BC Helix is reached.

503 Perhaps surprisingly, the optimal untwisting is accomplished only by changing the length  
504 of the two-hop member, leaving the one-hop member and rail length equivalent within this  
505 continuum.<sup>2</sup> However, it should be noted that an engineer or architect may also use  $\mathbf{H}_{general}$   
506 directly and interactively via <https://pubinv.github.io/tetrahelix/>, and that minimax length  
507 optimality is a mathematical starting point rather than the final word on the beauty and  
508 utility of physical structures. For example, a structural engineer might increase radius past  
509 optimality in order to resist buckling.

510 If an equitetrabeam were actually used as a beam, an engineer might start with the optimal  
511 tetrabeam and dilate it in one dimension to stiffen the beam by deepening it. Similarly, simple  
512 length changes curve the equitetrabeam into an arch. The “colored” approach of (7) exposes  
513 these possibilities more than the approach of (1).

514 Trusses and space frames remain an important design field in mechanical and structural  
515 engineering[10], including deployable and moving trusses[2].

---

<sup>2</sup>Before deriving Equation (9), we created a continuum by using a linear interpolation between the optimal radius for the Equitetrabeam and the BC Helix. This minimax optimum of this simpler approach was at most 1% worse than the optimum computed by (9).

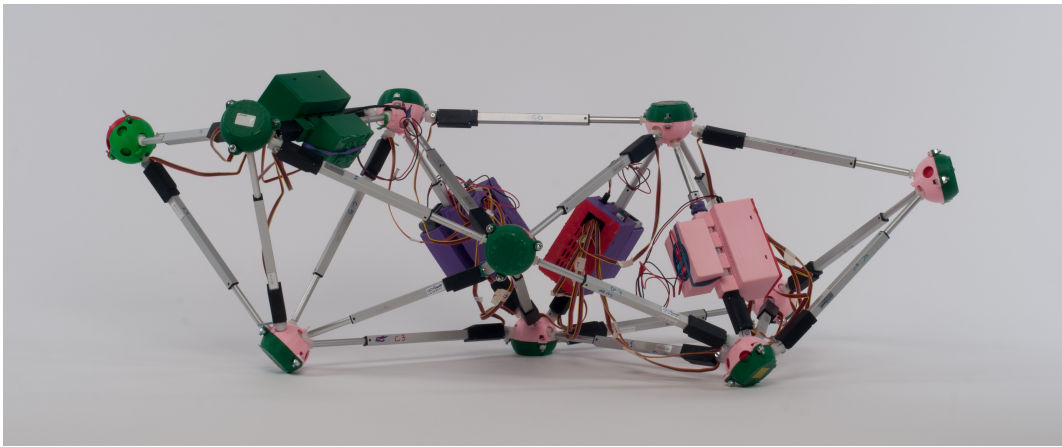


**Figure 11.** 7-Tet Tetrobot in relaxed, or BC helix configuration

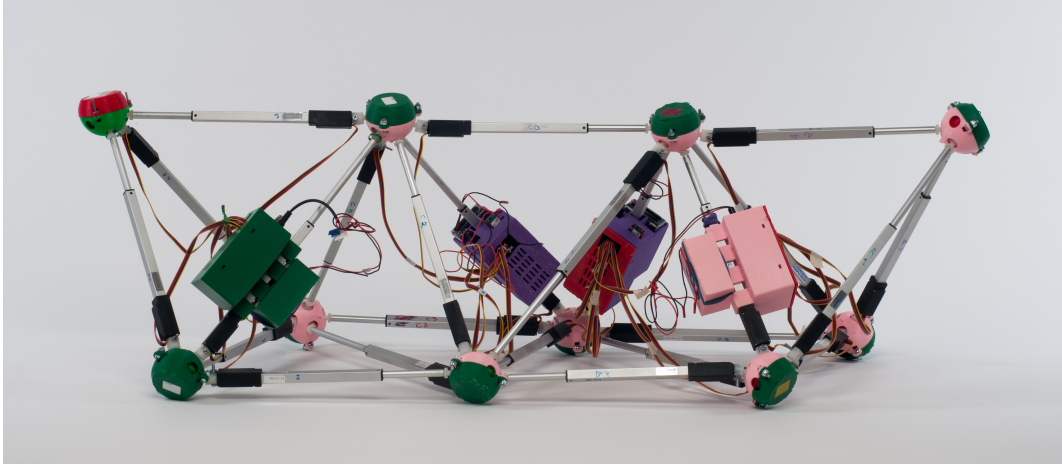


**Figure 12.** The Equitetrabeam: Fully Untwisted 7-Tet Tetrobot in Hexapod Configuration

516     **8. Utility for Robotics.** Starting twenty years ago, Sanderson[14], Hamlin,[8], Lee[9], and  
 517     others created a style of robotics based on changing the lengths of members joined at the  
 518     center of a joint, thereby creating a connection to pure geometry. More recently NASA has  
 519     experimented with tensegrities[1], a different point in the same design spectrum.

520     As suggested by Buckminster Fuller, the most convenient geometries to consider are those  
 521     that have regular member lengths, in order to facilitate the inexpensive manufacture and  
 522     construction of the robot. In a plane, the octet truss[4] is such a geometry, but in a line, the  
 523     Boerdijk-Coxeter helix is a regular structure.

524     However, a robot must move, and so it is interesting to consider the transmutations of  
 525     these geometries, which was in fact the motivation for creating the equitetrabeam.

526     **Theorem 7.** *By changing only the length of the longer members that connect two distinct  
 527     rails (the two-hop members), we can dynamically untwist a tetrobot forming the Boerdijk-  
 528     Coxeter configuration into the equitetrabeam which rests flat on the plane.*

529     *Proof.* Proof by our computer program that does this using Equation (7) applied to the  
530 physical 7-tet Tetrobot.

531     By untwisting the tetrahelix so that it has a planar surface resting on the ground, we may  
532 consider each vertex touching the ground a foot or pseudopod. A robot can thus become a  
533 hexapod or  $n$ -pod robot, and the already well-developed approaches to hexapod gaits may be  
534 applied to make the robot walk or crawl.

535     **9. Conclusion.** The BC Helix is the end point of a continuum of tetrahelices, the other end  
536 point being an untwisted tetrahelix with equilateral cross section, constructed by changing the  
537 length of only those members crossing the outside rails after hopping over the nearest vertex.  
538 Under the condition of minimum maximum length ratios of all members in the system, all  
539 such tetrahelices have vertices evenly spaced along the axis generated by a simple equation  
540 and are in fact triple helices. A machine, such as a robot or a variable-geometry truss, that  
541 can change the length of its members can thus twist and untwist itself by changing the length  
542 of the appropriate members to achieve any point in the continuum. With a numeric solution,  
543 a designer may choose a rotation angle and member lengths to obtain a desired pitch.

544     **10. Contact and Getting Involved.** The Tetrobot Project <http://pubinv.github.io/gluss/>  
545 is part of Public Invention <https://pubinv.github.io/PubInv/>, a free-libre, open-source re-  
546 search, hardware, and software project that welcomes volunteers. To assist, contact  
547 [read.robert@gmail.com](mailto:read.robert@gmail.com).

548

## REFERENCES

- 549 [1] *NTRT - NASA Tensegrity Robotics Toolkit.* <https://ti.arc.nasa.gov/tech/asr/intelligent-robotics/tensegrity/ntrt/>. Accessed: 2016-09-13.
- 550 [2] J. CLAYPOOL, *Readily configured and reconfigured structural trusses based on tetrahedrons as modules*, Sept. 18 2012, <https://www.google.com/patents/US8266864>. US Patent 8,266,864.
- 551 [3] H. COXETER ET AL., *The simplicial helix and the equation  $\tan(n \theta) = n \tan(\theta)$* , Canad. Math. Bull, 28 (1985), pp. 385–393.
- 552 [4] R. FULLER, *Synergetic building construction*, May 30 1961, <https://www.google.com/patents/US2986241>. US Patent 2,986,241.
- 553 [5] R. FULLER AND E. APPLEWHITE, *Synergetics: explorations in the geometry of thinking*, Macmillan, 1982, <https://books.google.com/books?id=G8baAAAAMAAJ>.
- 554 [6] R. W. GRAY, *Tetrahelix data*. <http://www.rwgrayprojects.com/rbfnotes/helix/helix01.html>, <http://www.rwgrayprojects.com/rbfnotes/helix/helix01.html> (accessed Accessed: 2017-04-08).
- 555 [7] G. J. HAMLIN AND A. C. SANDERSON, *A novel concentric multilink spherical joint with parallel robotics applications*, in Proceedings of the 1994 IEEE International Conference on Robotics and Automation, May 1994, pp. 1267–1272 vol.2, <https://doi.org/10.1109/ROBOT.1994.351313>.
- 556 [8] G. J. HAMLIN AND A. C. SANDERSON, *Tetrobot: A Modular Approach to Reconfigurable Parallel Robotics*, Springer Science & Business Media, 2013, <https://play.google.com/store/books/details?id=izrSBwAAQBAJ> (accessed 2017-04-08).
- 557 [9] W. H. LEE AND A. C. SANDERSON, *Dynamic rolling locomotion and control of modular robots*, IEEE Transactions on robotics and automation, 18 (2002), pp. 32–41.
- 558 [10] M. MIKULAS AND R. CRAWFORD, *Sequentially deployable maneuverable tetrahedral beam*, Dec. 10 1985, <https://www.google.com/patents/US4557097>. US Patent 4,557,097.
- 559 [11] R. L. READ, *Gluss = Slug + Truss*. Unpublished preprint, <https://github.com/PubInv/tetrobot/blob/gh-pages/doc/Gluss.pdf> (accessed 2016-10-27).

- 573 [12] R. L. READ, *Untwisting the tetrahelix website*. <https://pubinv.github.io/tetrahelix/>, <https://pubinv.github.io/tetrahelix/> (accessed 2017-04-08).
- 574 [13] G. SADLER, F. FANG, J. KOVACS, AND K. IRWIN, *Periodic modification of the Boerdijk-Coxeter helix*  
575 (*tetrahelix*), arXiv preprint arXiv:1302.1174, (2013), <https://arxiv.org/abs/1302.1174>.
- 576 [14] A. C. SANDERSON, *Modular robotics: Design and examples*, in Emerging Technologies and Factory Au-  
577 tomation, 1996. EFTA'96. Proceedings., 1996 IEEE Conference on, vol. 2, IEEE, 1996, pp. 460–466.
- 578 [15] S. SONG, D. KWON, AND W. KIM, *Spherical joint for coupling three or more links together at one point*,  
579 May 27 2003, <http://www.google.com/patents/US6568871>. US Patent 6,568,871.
- 580